Environment International 187 (2024) 108668

Contents lists available at ScienceDirect

Environment International

journal homepage: www.elsevier.com/locate/envint

Full length article

Air pollution changes due to COVID-19 lockdowns and attributable mortality changes in four countries

Yiqun Ma[a,b,1], Federica Nobile[c,1], Anne Marb[d,e,1], Robert Dubrow[a,b], Patrick L. Kinney[f], Annette Peters[d,e], Massimo Stafoggia[c,2], Susanne Breitner[d,e,2], Kai Chen[a,b,2,*]

[a] *Department of Environmental Health Sciences, Yale School of Public Health, New Haven, CT, USA*
[b] *Yale Center on Climate Change and Health, Yale School of Public Health, New Haven, CT, USA*
[c] *Department of Epidemiology, Lazio Region Health Service / ASL Roma 1, Rome, Italy*
[d] *Chair of Epidemiology, IBE, Faculty of Medicine, LMU Munich, Munich, Germany*
[e] *Institute of Epidemiology, Helmholtz Zentrum München - German Research Center for Environmental Health, Neuherberg, Germany*
[f] *Department of Environmental Health, Boston University School of Public Health, Boston, MA, USA*

ARTICLE INFO

Handling Editor: Zorana Andersen

Keywords:
Air pollution
COVID-19
Lockdown
Mortality

ABSTRACT

COVID-19 lockdowns reduced nitrogen dioxide (NO_2) and fine particulate matter ($PM_{2.5}$) emissions in many countries. We aim to quantify the changes in these pollutants and to assess the attributable changes in mortality in Jiangsu, China; California, U.S.; Central-southern Italy; and Germany during COVID-19 lockdowns in early 2020. Accounting for meteorological impacts and air pollution time trends, we use a machine learning-based meteorological normalization technique and the difference-in-differences approach to quantify the changes in NO_2 and $PM_{2.5}$ concentrations due to lockdowns. Using region-specific estimates of the association between air pollution and mortality derived from a causal modeling approach using data from 2015 to 2019, we assess the changes in mortality attributable to the air pollution changes caused by the lockdowns in early 2020. During the lockdowns, NO_2 reductions avoided 1.41 (95% empirical confidence interval [eCI]: 0.94, 1.88), 0.44 (95% eCI: 0.17, 0.71), and 4.66 (95% eCI: 2.03, 7.44) deaths per 100,000 people in Jiangsu, China; California, U.S.; and Central-southern Italy, respectively. Mortality benefits attributable to $PM_{2.5}$ reductions were also significant, albeit of a smaller magnitude. For Germany, the mortality benefits attributable to NO_2 changes were not significant (0.11; 95% eCI: −0.03, 0.25), and an increase in $PM_{2.5}$ concentrations was associated with an increase in mortality of 0.35 (95% eCI: 0.22, 0.48) deaths per 100,000 people during the lockdown. COVID-19 lockdowns overall improved air quality and brought attributable health benefits, especially associated with NO_2 improvements, with notable heterogeneity across regions. This study underscores the importance of accounting for local characteristics when policymakers adapt successful emission control strategies from other regions.

1. Introduction

Unprecedented public health interventions were implemented worldwide in early 2020 to control the COVID-19 pandemic. The decrease in transportation and non-essential business activities during the COVID-19 lockdowns temporarily led to a substantial reduction in air pollution in many countries, particularly nitrogen dioxide (NO_2) and, to a lesser degree, fine particulate matter ($PM_{2.5}$) (Shi et al., 2021; Venter et al., 2020; Zhang et al., 2022). Ambient air pollution is the leading environmental risk factor for mortality, contributing to over 4.5 million deaths globally in 2019 (GBD 2019 Risk Factors Collaborators, 2020). Therefore, the large-scale lockdown policies in early 2020 provided a unique opportunity to assess the impacts of reduced air pollution on mortality in regions with varying air pollution levels and socioeconomic statuses where mortality was only mildly impacted by the early stages of the pandemic itself.

Previous studies have assessed the mortality benefits attributable to air pollution reductions during COVID-19 lockdowns (Achebak et al., 2021; Chen et al., 2020; Giani et al., 2020; Son et al., 2020). However, the reported attributable mortality benefits from these studies were

* Corresponding authors at: Yale School of Public Health, 60 College Street, New Haven, CT 06520-8034, USA.
E-mail address: kai.chen@yale.edu (K. Chen).
[1] Contributed equally.
[2] Joint last authors.

https://doi.org/10.1016/j.envint.2024.108668
Received 29 November 2023; Received in revised form 20 March 2024; Accepted 15 April 2024
Available online 16 April 2024

inconsistent in magnitude. In addition to the variation in the duration of the lockdown period across studies, the disparity in estimates mainly derived from two aspects of the assessment process: first, the quantification of air pollution changes due to lockdowns, and second, the selection of exposure–response functions (ERFs) to characterize the relationship between air pollution and mortality. Both elements make it challenging to accurately assess the attributable mortality benefits.

One common approach to quantify air pollution changes due to COVID-19 lockdowns is the difference-in-differences (DiD) analysis (Chen et al., 2020; Shi et al., 2021; Son et al., 2020). This approach, which compares the air pollution changes before and after the implementation of lockdowns versus the corresponding changes in the same calendar periods in previous years, controls for the long-term trend and seasonality of air pollution (Chen et al., 2020; Shi et al., 2021). Removing these impacts is essential because air quality levels typically vary from winter to spring (seasonality) and, in some countries, present a long-term decreasing trend due to air pollution mitigation policies in recent years (long-term trend). However, air pollution changes estimated with the DiD analysis cannot be fully attributed to the lockdown because this approach does not fully control for the influences of meteorological conditions (Achebak et al., 2020). Failing to decouple the meteorological impacts may lead to a biased estimate of air pollution changes due to lockdowns.

Utilizing ERFs from existing epidemiological literature is a common practice in studies assessing the health impacts of lockdown-related air pollution changes. However, substantial spatial heterogeneity in ERFs exists (Chen et al., 2018; Liu et al., 2019; Meng et al., 2021), especially between developed and developing countries and between low-polluted and high-polluted regions (Chen et al., 2018; Liu et al., 2019). In addition, the association between short-term air pollution exposure and health outcomes can vary over time in the long run (Chen et al., 2021a). Therefore, using localized ERFs from recent data is important when assessing the mortality benefits attributable to air pollution changes due to the lockdowns.

This study aims first to quantify the changes in NO_2 and $PM_{2.5}$ due to COVID-19 lockdowns in early 2020 and then to assess the impacts of these air pollution changes on mortality in Jiangsu Province, China; California, U.S.; Central-southern Italy; and Germany, four regions that implemented lockdowns but were not severely affected by the pandemic in early 2020. We utilized a machine-learning-based meteorological normalization technique (Grange and Carslaw, 2019; Grange et al., 2018) to account for the meteorological impacts; used the DiD approach to control for time trends in the quantification of air pollution changes due to the lockdowns; and applied region-specific ERFs estimated from recent data using a causal inference approach in the assessment of attributable mortality impacts.

2. Material and methods

2.1. Study regions

To reduce the impact of COVID-19 deaths and the disruption and overload in healthcare systems, this study focused on four regions where air pollution and mortality data were available, and which implemented COVID-19 lockdown measures but were in general not severely affected by the COVID-19 pandemic in early 2020: Jiangsu Province in China, California in the U.S., Central-southern Italy, and Germany. To assess the severity of COVID-19 impacts, we mapped the excess mortality during the COVID-19 outbreak in early 2020 using a two-stage interrupted time-series analysis (Scortichini et al., 2020) and found that each region had a relatively small COVID-19 mortality burden (**Methods S1**; Northern Italy was excluded due to its high excess mortality). The region-specific spatial units used in this study were counties in Jiangsu, China; California, U.S.; and Germany; and municipalities in Central-southern Italy, which were the finest possible administrative units where mortality data were accessible in each region.

2.2. COVID-19 lockdown period

In the main analysis, we defined the COVID-19 lockdown period in each region using the start and end dates of national and regional lockdown policies that included stay-at-home requirements, strict travel restrictions, and closure of non-essential businesses: January 31 – March 14, 2020 in Jiangsu, China; March 19 – May 07, 2020 in California, U.S.; March 09 – May 04, 2020 in Central-southern Italy; and March 22 – May 04, 2020 in Germany. Details of the region-specific lockdown policy timelines are described in **Methods S2**.

Given that behavioral changes in response to the COVID-19 pandemic might have started before official lockdown policies were implemented and might continue after the policies ended, we utilized mobility data to define alternative lockdown periods as a sensitivity analysis. The data sources for mobility data, the calculation process, and the defined mobility-based lockdown periods are described in detail in **Methods S3**.

2.3. Air pollution and meteorological data

Hourly site-specific NO_2 and $PM_{2.5}$ monitoring data from 2015 to 2020 were obtained from the China National Air Pollution Monitoring System for Jiangsu, China; the U.S. EPA Air Quality System for California, U.S.; and the official monitoring network of the German Environment Agency for Germany. For Central-southern Italy, we collected NO_2 and $PM_{2.5}$ monitoring data with daily resolution from the Italian Institute of Environmental Research and Protection because hourly data were available for only 6.54 % of $PM_{2.5}$ monitoring sites, and we aimed to maintain a consistent temporal resolution for both air pollutants. The number of monitoring sites and spatial units with monitoring sites are listed in **Table S1**.

Hourly meteorological variables, including 2 m temperature, 2 m dew temperature, boundary layer height, total precipitation, surface pressure, surface net solar radiation, surface solar radiation downwards, downward UV radiation at the surface, total cloud cover, 10 m u-component of wind, 10 m u-component of neutral wind, 10 m v-component of wind, and 10 m v-component of neutral wind, were obtained from the fifth-generation European Centre for Medium-Range Weather Forecasts atmospheric reanalysis of the global climate (ERA5) dataset (Hersbach et al., 2018). Meteorological data were extracted using the geographic coordinates of air quality monitoring sites and matched to the site-specific records of NO_2 and $PM_{2.5}$ concentrations in each study region.

2.4. Meteorological normalization

Rapidly changing meteorological conditions may affect air pollutant concentrations even when emissions remain the same. Therefore, we applied a machine learning-based meteorological normalization technique to disentangle the impacts of meteorological conditions (Grange and Carslaw, 2019; Shi et al., 2021). The meteorological normalization was performed at the hourly and site-level for Jiangsu, China; California, U.S.; and Germany, and on the daily and site-level for Central-southern Italy due to the unavailability of hourly $PM_{2.5}$ concentrations in most Italian monitoring stations. We first developed a Random Forest (RF) model independently for each pollutant and January to May each year (2015 to 2020), in each spatial unit where one or multiple monitoring sites were located, within each study region. Seventy percent of the dataset was randomly selected to train the RF model, and the remaining 30 % were used to evaluate the performance of the trained model. Predictors included time variables (Unix time, Julian day, day of the week, and hour of the day), location (longitude, latitude), and all meteorological variables obtained from the ERA5 reanalysis dataset. In terms of the hyperparameters of the RF model, the number of trees was set to 300, the minimum node size was 5, and the number of variables that may split at each node was set to 4. We set these parameters based on the model settings from a previous study, without performing tuning, because the models were found to be insensitive to the choice of parameters (Grange et al., 2018). Model performance was evaluated using coefficient of determination (R^2) and root mean square error (RMSE) in the testing dataset with a daily resolution.

The meteorological normalization of the air pollution time series was achieved by repeatedly sampling meteorological factors and making predictions using the trained RF models for each year and each spatial unit. We randomly resampled the meteorological factors from the whole study period without replacement 1000 times, producing 1000 model predictions for each air pollution observation. These predictions were then aggregated using the arithmetic mean to obtain the deweathered air pollution concentration, representing the expected air pollution level when the meteorological conditions were "average" (Shi et al., 2021). Finally, we calculated the daily deweathered air pollution concentrations in each spatial unit by averaging the hourly site-specific data for Jiangsu, China; California, U.S.; and Germany, and daily site-specific data for Central-southern Italy.

2.5. Difference-in-differences analysis

After decoupling the impacts of varying meteorological conditions, we applied a DiD analysis to further account for long-term and seasonal air pollution trends when quantifying the air pollution changes due to the COVID-19 lockdowns. Specifically, for each study region, we calculated spatial-unit-specific changes in average deweathered air pollution concentrations during the COVID-19 lockdown versus a reference period before the lockdown in early 2020 (defined below). We then compared these changes with changes between the corresponding calendar periods during 2015 to 2019. This process was repeated for all 1000 samples of the deweathered air pollution concentrations to calculate the 95 % empirical confidence intervals (95 % eCIs) of the air pollution changes due to the lockdowns based on the 2.5th and 97.5th percentiles of the distribution of the results.

We defined the reference period as January 1, 2020 to seven days before the lockdown in each region started. The seven days immediately preceding the lockdowns were excluded because this period was considered a transition period. In a sensitivity analysis, we used two alternative reference periods: a 21-day period ending seven days before the start of the lockdown and a period of the same duration as the lockdown ending seven days before the lockdown (**Methods S4**).

2.6. Assessment of mortality changes attributable to lockdown-induced air pollution changes

To assess the mortality changes attributable to lockdown-induced air pollution changes, we obtained region-specific associations between short-term changes in $PM_{2.5}$ and NO_2 concentrations and changes in daily all-cause mortality rates on lag 01 or 02 days from a previous study (Ma et al., 2024). In brief, the ERFs were estimated using 2015–2019 data separately for Jiangsu, China; California, U.S.; Central-southern Italy; and Germany, utilizing an interactive fixed effects (IFE) model. The IFE model, a causal modeling approach, accounted for unmeasured time-varying confounders across different spatial units by decomposing them into common time-varying factors with corresponding unobserved spatial unit level loading parameters (Ma et al., 2024) (see details in **Methods S5**). The coefficient of the IFE model can be interpreted as the change in the daily mortality rate for each unit change in the daily air pollution level, which was suitable for the purpose of the current study. The ERFs from the single-pollutant models were used in the main analysis, and we utilized the two-pollutant model ERFs in a sensitivity analysis. Spatial-unit-level population data in 2020 were collected from the official departments of each study region (**Table S2**).

For each study region, we calculated the attributable change in total mortality during the lockdown period in each spatial unit as follows:

$$\Delta Mortality_i = \beta \Delta Air\ pollution_i \times Number\ of\ lockdown\ days$$

$\Delta Mortality_i$ is the mortality change attributable to the air pollution change during the lockdown in spatial unit *i*. β is the region-specific association between short-term changes in $PM_{2.5}$ or NO_2 concentrations and changes in the daily all-cause mortality rate. $\Delta Air\ pollution_i$ is the quantified air pollution change due to the lockdown in spatial unit *i*. *Number of lockdown days* is the duration of COVID-19 lockdown period in each study region. We calculated the 95 % eCIs using Monte Carlo simulations (n = 10,000) based on the distribution of estimates of ERFs and air pollution changes. We also conducted a stratified analysis of urban versus rural spatial units to explore potential urban/rural differences in attributable mortality changes.

2.7. Sensitivity analysis

We performed several sensitivity analyses to test the robustness of our estimated air pollution changes due to the lockdown and the associated impacts on mortality: (a) we used mobility-based lockdown periods instead of policy-based lockdown periods; (b) we used two alternative reference periods in the DiD analysis; and (c) we applied the ERFs from two-pollutant models instead of single-pollutant models in the estimation of attributable mortality changes.

3. Results

3.1. Description of air pollution in early 2020

This study covered over 27 million people in Jiangsu, China; 37 million in California, U.S.; 13 million in Central-southern Italy; and 55 million in Germany. During the reference period in 2020, the average daily NO_2 concentration ranged from 20.3 μg/m^3 in Germany to 40.3 μg/m^3 in Jiangsu, China; and the average daily $PM_{2.5}$ concentration ranged from 8.2 μg/m^3 in California, U.S. to 72.1 μg/m^3 in Jiangsu, China. Compared to the reference period, the average concentrations of both NO_2 and $PM_{2.5}$ were lower in the lockdown period in all study regions, except for $PM_{2.5}$ in Germany (**Table S3**). However, this simple comparison cannot demonstrate that COVID-19 lockdowns reduced air pollution because both seasonality and meteorological conditions affect air pollution changes.

3.2. Air pollution changes due to COVID-19 lockdowns

The RF models demonstrated satisfactory performance, with an $R^2 \geq$ 0.80 for all years in Jiangsu, China; California, U.S.; and Germany, and an $R^2 \geq 0.60$ for NO_2 and ≥ 0.50 for $PM_{2.5}$ for all years in Central-southern Italy (**Table S4**).

The temporal trends in deweathered air pollution concentrations were much smoother than the trends in observed concentrations, as the impacts from daily weather variations were normalized (**Fig. S1**). Fig. 1 shows the time series of the observed and deweathered air pollution concentrations from January to May 2020 and the average concentrations in the same calendar period from 2015 to 2019 in all four study regions. The overall decreasing trends of 2015–2019 deweathered NO_2 and $PM_{2.5}$ concentrations from January to May in all study regions indicated the seasonality of air pollution. In addition, in all regions, especially Jiangsu, China and Germany, the concentrations of both observed and deweathered NO_2 were consistently higher from 2015 to 2019 compared to 2020, even in the reference period, indicating a long-term decreasing trend.

Using DiD analyses to further account for these long-term and seasonal trends, we calculated the air pollution changes due to the lockdown in each spatial unit in each region (Fig. 2). We observed significant reductions in average daily mean NO_2 concentrations due to COVID-19 lockdowns in all study regions except Germany: −8.98 (95 % eCI: −9.67,

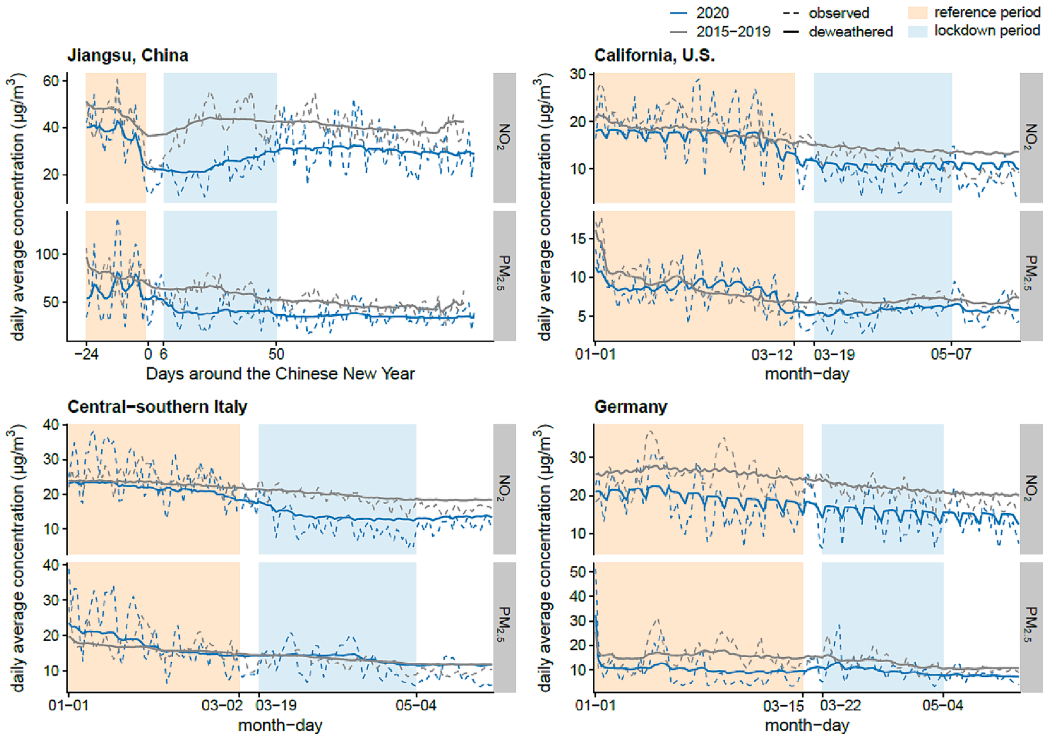

Fig. 1. Observed and deweathered daily NO_2 and $PM_{2.5}$ concentrations in all four study regions from January to May of 2020 versus 2015–2019 This figure displays the time-series of the observed and deweathered air pollution concentrations in January to May 2020 and the average concentration in the same calendar period from 2015 to 2019 in all four study regions. For Jiangsu, China, we used Chinese lunar calendar dates to account for the Chinese New Year holiday.

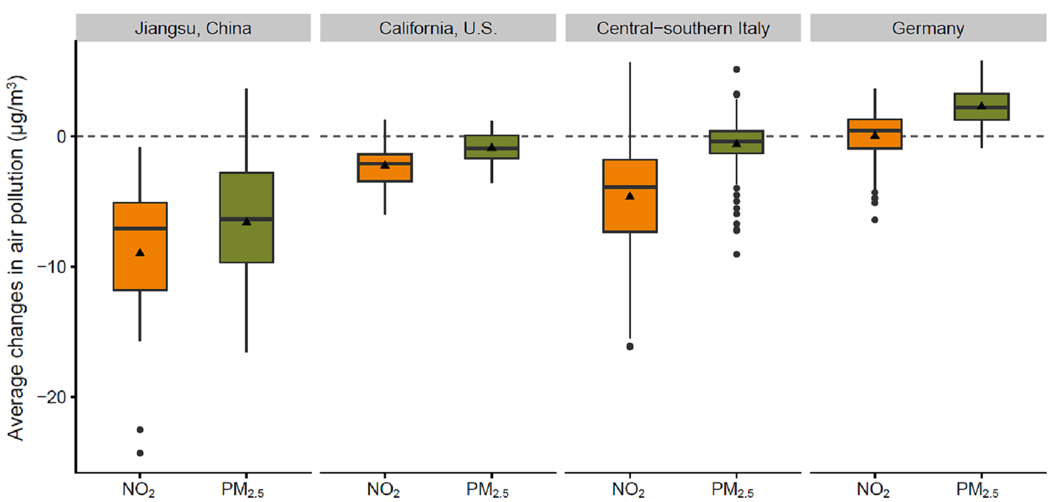

Fig. 2. Distribution of spatial-unit-level changes in average daily mean NO_2 and $PM_{2.5}$ concentrations due to the COVID-19 lockdown in each region These box plots show the distribution of spatial-unit-level changes in average daily mean NO_2 and $PM_{2.5}$ concentrations (μg/m^3) due to the COVID-19 lockdown in each study region. Lower and upper box boundaries represent the 25th and 75th percentiles of the distribution; lower and upper error lines represent 1.5 interquartile range below the third quartile and above the first quartile; the horizontal line and triangle inside boxes represent median and mean values, respectively. The black dots represent outliers.

−8.30) μg/m^3 in Jiangsu, China; −2.27 (95 % eCI: −2.65, −1.88) μg/m^3 in California, U.S.; −4.65 (95 % eCI: −6.26, −3.04) μg/m^3 in Central-southern Italy; and 0.02 μg/m^3 (95 % eCI: −0.46, 0.51) in Germany. We estimated smaller reductions in average daily $PM_{2.5}$ concentrations of −6.62 (95 % eCI: −7.75, −5.49) μg/m^3 in Jiangsu, China; −0.90 (95 % eCI: −1.05, −0.75) μg/m^3 in California, U.S.; and −0.63 (95 % eCI: −2.14, 0.88) μg/m^3 in Central-southern Italy. For Germany, the average daily $PM_{2.5}$ level increased significantly by 2.27 (95 % eCI: 1.91, 2.63) μg/m^3.

Fig. 3 displays the spatial distribution of average daily air pollution changes due to the lockdowns in each study region. Except for the relatively consistent reduction in NO_2 and $PM_{2.5}$ concentrations in all studied counties in Jiangsu, China, a mixed spatial pattern was observed for both air pollutants in all other study regions. We observed significantly larger reductions in NO_2 and $PM_{2.5}$ concentrations in urban versus rural areas of California, U.S. and Central-southern Italy ($P < 0.05$). In Germany, urban counties experienced a reduction in NO_2, whereas rural counties had an increase; in addition, the increase in $PM_{2.5}$ in urban counties was significantly smaller than in rural counties (Table S5). We could not assess the urban–rural difference in Jiangsu,

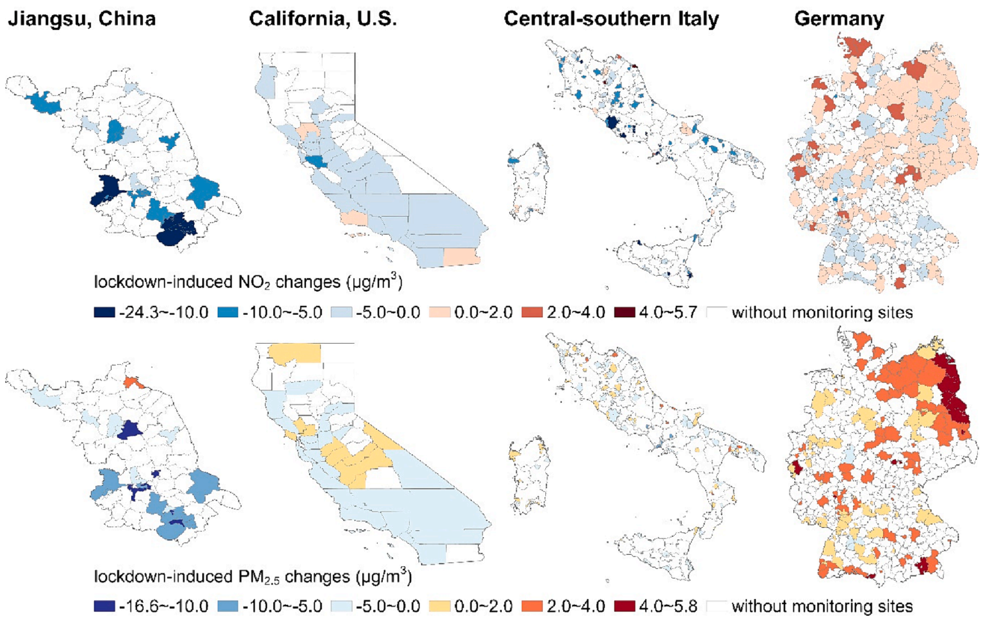

Fig. 3. Spatial distribution of the changes in average daily mean NO_2 and $PM_{2.5}$ concentrations due to the COVID-19 lockdown in each study region These maps display the spatial distribution of the changes in NO_2 and $PM_{2.5}$ concentrations (μg/m^3) due to the lockdown in each spatial unit in each study region. Blank areas represent spatial units that were excluded from our analysis due to the lack of air quality monitoring sites.

China because only three rural counties had air quality monitoring sites.

Sensitivity analyses showed that our estimated air pollution changes due to the lockdowns remain robust when using mobility-based lockdown periods and alternative reference periods (Fig. S2&S3). The magnitude of estimated air pollution changes was larger when we directly used observed air pollution data without weather normalization, indicating the necessity of disentangling the changes due to meteorological variation (Fig. S4).

3.3. Mortality changes attributable to lockdown-induced air pollution changes

Fig. 4 shows the estimated mortality changes attributable to NO_2 and $PM_{2.5}$ changes due to the lockdown in each study region. We estimated that the mortality changes attributable to NO_2 reductions due to the lockdowns were −1.41 (95 %eCI: −1.88, −0.94) deaths per 100,000 people in Jiangsu, China; −0.44 (95 % eCI: −0.71, −0.17) deaths per 100,000 people in California, U.S.; and −4.66 (95 % eCI: −7.44, −2.03) deaths per 100,000 people in Central-southern Italy. Smaller mortality benefits from $PM_{2.5}$ reduction were observed in these three regions: −0.16 (95 % eCI: −0.29, −0.04) deaths, −0.23 (95 % eCI: −0.43, −0.03) deaths, and −0.91 (95 % eCI: −1.78, −0.09) deaths per 100,000 people in Jiangsu, China; California, U.S.; and Central-southern Italy, respectively. For Germany, the mortality benefit attributable to NO_2 changes during the lockdown was not statistically significant (−0.11 deaths per 100,000 people; 95 % eCI: −0.25, 0.03), and $PM_{2.5}$ changes were associated with an increase in mortality burden by 0.35 (95 % eCI: 0.22, 0.48) deaths per 100,000 people. The total changes in mortality count in each region can be found in Table S6.

The maps of attributable mortality changes are shown in Fig. 5. NO_2 changes due to the COVID-19 lockdowns were associated with mortality benefits for all spatial units in Jiangsu, China; most spatial units in California, U.S. and Central-southern Italy; and some counties, mostly urban, in Germany. Mortality benefits attributable to $PM_{2.5}$ changes

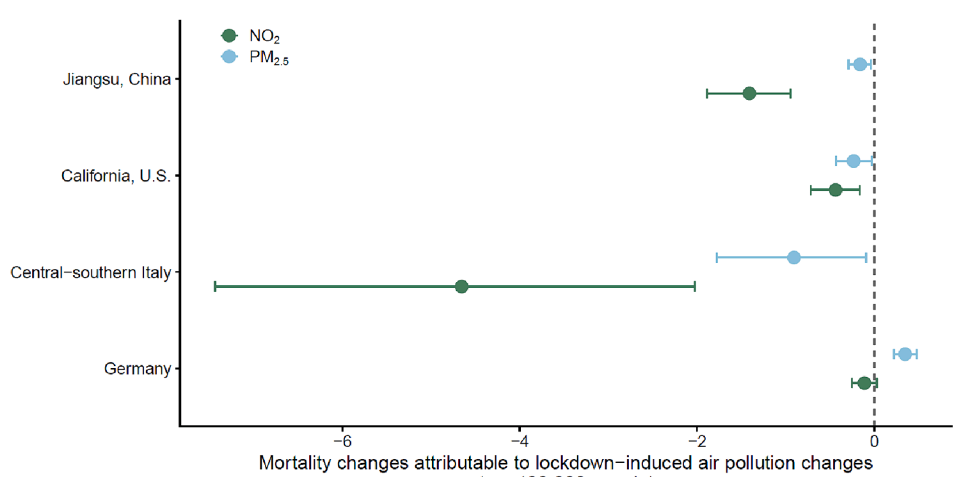

Fig. 4. Mortality changes attributable to air pollution changes due to COVID-19 lockdown in each region (per 100,000 people) This plot presents the estimated changes in mortality (per 100,000 people) attributable to NO_2 and $PM_{2.5}$ changes due to the lockdown in each study region. The error bars present the 95% confidence intervals.

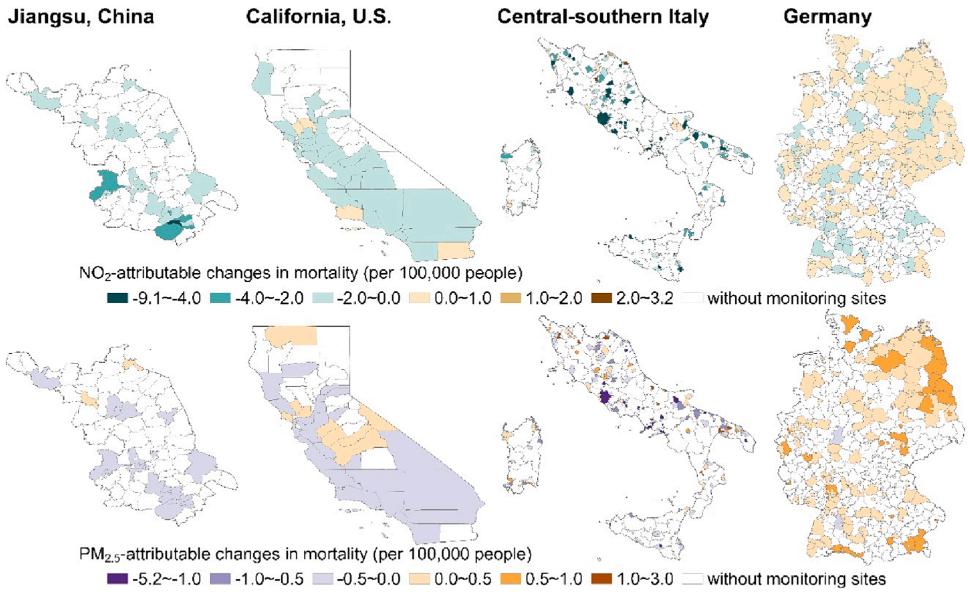

Fig. 5. Spatial distribution of mortality changes attributable to air pollution changes due to the lockdown in each study region (per 100,000 people) These maps display the spatial distribution of the changes in mortality (per 100,000 people) attributable to NO_2 and $PM_{2.5}$ changes due to the lockdown in each spatial unit in each study region. Blank areas represent spatial units that were excluded from our analysis due to the lack of air quality monitoring sites.

were found for most spatial units in Jiangsu, China; California, U.S.; and Central-southern Italy, while the $PM_{2.5}$-attributable mortality burden in most German counties increased. Consistent with the findings for lockdown-induced air pollution changes, larger mortality benefits attributable to changes in NO_2 and $PM_{2.5}$ concentrations were observed in urban versus rural areas of California, U.S., and Central-southern Italy ($P < 0.05$). In Germany, a reduction in NO_2-attributable mortality was found in urban counties, in contrast to the increase in rural counties; the increase in mortality burden attributable to increases in $PM_{2.5}$ was significantly smaller in urban counties than in rural counties ($P = 0.018$) (**Table S7**).

In sensitivity analyses, the estimated attributable mortality impacts generally remained robust when using mobility-based lockdown periods, alternative reference periods, and the ERFs from two-pollutant models instead of single-pollutant models (**Fig. S5&S6**, **Table S8**).

4. Discussion

Utilizing deweathered and detrended air pollution data and the most recent and localized estimations of the air pollution-mortality relationship, we reported relevant mortality benefits brought by air pollution reduction due to the lockdowns in Jiangsu, China; California, U.S.; and Central-southern Italy, with smaller magnitudes from $PM_{2.5}$ reduction compared to NO_2. In Germany, we found an increase in $PM_{2.5}$-attributable mortality burden during the lockdown and no significant impact on mortality from changes in NO_2.

We observed meaningful reductions in NO_2 and $PM_{2.5}$ concentrations due to the lockdowns in Jiangsu, China; California, U.S.; and Central-southern Italy, which led to mortality benefits in these regions. Lockdown-induced NO_2 and $PM_{2.5}$ reductions avoided approximately 0.4 to 4.6 and 0.2 to 0.9 deaths per 100,000 people in these three regions, respectively. These magnitudes are greater than the global monthly mortality rate for brain cancer (0.3 per 100,000 people) and kidney cancer (0.2 per 100,000 people) in 2019 (GBD 2019 Risk Factors Collaborators, 2020). This finding is generally consistent with most previous single- or multi-location studies in China (Chen et al., 2021b; Chen et al., 2020), the U.S. (Son et al., 2020), and Europe (Achebak et al., 2021; Giani et al., 2020; Schneider et al., 2022). For example, a previous study reported a 10.05 $\mu g/m^3$ decrease in $PM_{2.5}$ during the lockdown nationwide in China, which was associated with a reduction of 2.01 deaths per 100,000 people in Jiangsu (Chen et al., 2021b). Another study in the U.S. found that $PM_{2.5}$ decreased by 4.20 $\mu g/m^3$ during the lockdown in California, which avoided approximately 1.27 deaths per 100,000 people (Son et al., 2020). However, a direct comparison across studies is challenging due to differences in spatial coverage, administrative levels, reference periods, definitions of lockdown, and baseline mortality rates. The magnitudes of our study's estimated air pollution reductions are lower than many of those previously reported (Chen et al., 2021b; Giani et al., 2020; Son et al., 2020), which may be explained by the weather normalization. The difference between our estimated region-specific ERFs and those obtained from global epidemiological studies (Liu et al., 2019; Meng et al., 2021) also contributed to the difference in the estimated attributable mortality benefits. In addition, like previous studies, this study analyzed the changes in NO_2 and $PM_{2.5}$ and the associated mortality changes separately to provide full information for individual pollutants; therefore, the estimated mortality changes attributable to these pollutants cannot be summed up due to the potential overlap in their impacts.

In Germany, we observed no overall significant NO_2 reduction and a slight increase in $PM_{2.5}$ during the lockdown in early 2020. This unexpected finding may be explained by both local emissions and long-range atmospheric transport. First, although the COVID-19 lockdown in Germany reduced traffic overall, the number of medium and large trucks on the road remained almost unchanged, the public transport system was still operating, and the volume of delivery traffic may have increased (German Environment Agency, 2021). In addition, emission sources other than traffic, such as wood heating, energy production, and agriculture, were unaffected (Herrmann et al., 2020). Second, long-range atmospheric transport of polluted air masses containing particulate matter reached Germany during the lockdown, including particles from forest and land fires in Eastern Europe in March and April (Herrmann et al., 2020) and Saharan dust from North Africa in March (but not Italy) (German Environment Agency, 2021). The magnitude of this pollution may have been equal to or greater than the magnitude of the local emissions reductions due to the lockdown. An increase in average $PM_{2.5}$ concentrations during the lockdown was also observed in some other European cities, such as Prague, Brussels, and Copenhagen (Putaud et al., 2023). The results of our study are generally consistent with a previous single-city study in Augsburg, Germany: Cao et al. reported changes of -5.40 $\mu g/m^3$ in NO_2 and 1.37 $\mu g/m^3$ in $PM_{2.5}$ during the first lockdown (Cao et al., 2022); in our study, the estimated change in Augsburg was −2.24 μg/m^3 for NO_2 and 1.52 μg/m^3 for $PM_{2.5}$. Moreover, our study found a reduction in NO_2, especially in urban counties, in contrast to an increase in rural counties. Furthermore, the increases in $PM_{2.5}$ were significantly smaller in urban counties than in rural counties.

The heterogeneous results in different study regions in our study highlight the need for localized studies to assess the effects of COVID-19 lockdowns on air quality and the attributable health impacts. Multiple factors, such as the stringency of COVID-19 containment response policies, the dominant emission sectors, population density, baseline air pollution level, socioeconomic factors, and regional economic activity, can influence the impacts of lockdowns on air quality changes (Bluhm et al., 2022; Giani et al., 2020; Zhang et al., 2022). The associations between air pollution and health outcomes may also vary across regions due to different chemical compositions of air pollution mixtures, population characteristics related to susceptibility such as age structure, regional climate, and other factors (Samet, 2008). Using the COVID-19 lockdown as a natural experiment, this study underscores the importance of accounting for local characteristics when policymakers adapt successful emission control strategies from other regions. Designing effective environmental and public health policies tailored to their own regions is crucial, as these local factors largely influence the subsequent effects on air quality and the consequential health impacts.

The findings of our study could offer important insights into the local environmental and public health policies in each study region. For example, in Jiangsu, China, the air quality has greatly improved since the enactment of the National Air Quality Action Plan in 2013 (Zheng et al., 2024). However, air pollution levels in Jiangsu remain much higher compared to most regions in Europe and the U.S., with daily average NO_2 concentrations exceeding 40 μg/m^3 and $PM_{2.5}$ levels exceeding 70 μg/m^3 during the reference period in 2020. The notable reduction in air pollution and the subsequent decrease in mortality burden observed during the lockdown period suggest that adopting stricter air quality standards and continuing efforts to reduce air pollution could lead to substantial health benefits in Jiangsu in the future. California is among the states with the highest air pollution levels in the U.S., with traffic exhaust as a major source of air pollution, especially NO_2 (California Office of Environmental Health Hazard Assessment, 2022). Our study findings, along with evidence from previous studies (Parker et al., 2020; Yang et al., 2021), suggest that environmental policies aimed at mitigating traffic-related air pollution, such as reducing vehicular traffic and promoting public and active transportation methods, could yield meaningful environmental and public health benefits in California. In Italy, air pollution levels exhibit a slight decreasing trend over time (European Environment Agency, 2023b), although they are still high, particularly in the Northern regions and metropolitan areas such as Rome and Naples in Central-Southern Italy, where air pollution levels surpass the thresholds set by the latest WHO air quality guidelines (World Health Organization, 2021). Consequently, policies targeting the reduction of vehicular traffic and the overall mitigation of air pollutant emissions are needed to improve air quality, thereby yielding health benefits, as highlighted by other studies as well (Boniardi et al., 2022; Gualtieri et al., 2020). In Germany, both NO_2 and $PM_{2.5}$ concentrations have decreased in recent years, although NO_2 concentrations are still considerably higher in urban compared to rural areas (European Environment Agency, 2023a). During the COVID-19 lockdown, we observed a reduction in NO_2 levels especially in urban areas, which was associated with a mortality benefit. This highlights the need for further policies on mitigating ambient air pollution, such as reducing vehicular traffic or stricter emission control in areas with high levels of air pollution for greater public health benefits in Germany.

The strengths of this study included the selection of the first lockdown, its broad geographic scope, the use of deweathered and detrended air pollution data, and the application of region-specific ERFs estimated with recent data. First, we focused on the first lockdown period in response to the COVID-19 pandemic, which enabled us to identify regions less affected by the pandemic. Such a study became less feasible in subsequent lockdowns when COVID-19 cases skyrocketed with substantial mortality impacts from the pandemic. Second, this study included regions from four distinct countries, reflecting the influence of COVID-19 lockdowns in regions with varying air pollution levels and diverse socioeconomic backgrounds. Third, we utilized a machine-learning-based meteorological normalization technique to decouple the meteorological impacts, alongside the DiD approach to account for time trends when quantifying air pollution changes due to lockdowns. Finally, we applied the association between air pollution changes and mortality changes estimated using a causal inference approach with recent data specific to each study region to assess attributable mortality impacts.

Several limitations of this study should be noted. First, the spatial coverage within each study region was limited because we excluded spatial units where air quality monitoring stations were absent. Although approximately 96 % of the entire population of California, U.S. was included in the analysis, we only covered about 35 %, 54 %, and 67 % of the population in Jiangsu, China; Central-southern Italy; and Germany. Relying on air quality monitoring stations, we also were unable to fully capture variations within individual spatial units, which may be particularly pronounced for NO_2 (Cyrys et al., 2012; Xu et al., 2019). Other sources of air pollution data, such as highly spatially-resolved modeled data or low-cost air quality monitoring sensors, may be used in future studies to increase the spatial coverage. Second, although the meteorological normalization technique used in this study normalizes the impact of weather conditions on air quality, it does not account for (sudden) atmospheric long-distance transport, such as the Saharan dust event in Germany. Future studies should incorporate such transport processes in the analysis. Third, we selected regions that were only mildly impacted by the early stages of the COVID-19 pandemic to increase the applicability of ERFs estimated using pre-lockdown data (2015–2019). However, the relationship between air pollution and mortality could change during the lockdowns as human activity patterns change. Studies that examine the changes in air pollution-mortality relationships before and after the implementation of lockdowns are warranted. Fourth, we assumed that the ambient air pollution levels reflected individual exposures. This is a common assumption in air pollution epidemiology studies; however, this limitation becomes prominent in studies focusing on the lockdown period, when most people spent more time indoors. Further investigation is warranted into the personal or indoor air pollution exposure during the lockdowns.

5. Conclusions

In conclusion, this study documented meaningful improvements in air quality resulting from COVID-19 lockdowns and the associated mortality benefits in early 2020; however, notable heterogeneity existed across Jiangsu, China; California, U.S.; Central-southern Italy; and Germany. These findings offer robust scientific evidence to guide future air pollution mitigation and public health enhancement policies.

CRediT authorship contribution statement

Yiqun Ma: Writing – original draft, Visualization, Validation, Methodology, Investigation, Formal analysis, Data curation. **Federica Nobile:** Writing – original draft, Visualization, Validation, Investigation, Formal analysis. **Anne Marb:** Writing – original draft, Visualization, Validation, Investigation, Data curation, Formal analysis. **Robert Dubrow:** Writing – review & editing, Methodology, Investigation. **Patrick L. Kinney:** Writing – review & editing, Methodology, Investigation. **Annette Peters:** Methodology, Writing – review & editing. **Massimo Stafoggia:** Methodology, Investigation, Data curation, Conceptualization, Project administration, Supervision, Writing – review & editing. **Susanne Breitner:** Conceptualization, Data curation, Investigation, Methodology, Project administration, Supervision, Writing – review & editing. **Kai Chen:** Writing – review & editing, Validation, Supervision, Project administration, Methodology, Conceptualization, Data curation, Funding acquisition, Investigation.

Declaration of competing interest

The authors declare that they have no known competing financial interests or personal relationships that could have appeared to influence the work reported in this paper.

Data availability

The authors do not have permission to share data.

Acknowledgement

This work was supported by the Health Effects Institute (HEI) research agreement (grant No. 4984-RFA20-1B/21-7). The research described in this article was conducted under contract with the HEI, an organization jointly funded by the US Environmental Protection Agency (EPA) (assistance award No. R-82811201) and certain motor vehicle and engine manufacturers. The contents of this article do not necessarily reflect the views of the HEI or its sponsors, nor do they necessarily reflect the views and policies of the EPA or motor vehicle and engine manufacturers.

Appendix A. Supplementary material

Supplementary data to this article can be found online at https://doi.org/10.1016/j.envint.2024.108668.

References

Achebak, H., Petetin, H., Quijal-Zamorano, M., Bowdalo, D., García-Pando, C.P., Ballester, J., 2020. Reduction in air pollution and attributable mortality due to COVID-19 lockdown. Lancet Planet Health 4, e268.
Achebak, H., Petetin, H., Quijal-Zamorano, M., Bowdalo, D., García-Pando, C.P., Ballester, J., 2021. Trade-offs between short-term mortality attributable to NO2 and O3 changes during the COVID-19 lockdown across major Spanish cities. Environ. Pollut. 286, 117220.
German Environment Agency, 2021. Air Quality 2020 Preliminary Evaluation.
European Environment Agency, 2023a. Country fact sheet: Germany – air pollution country fact sheet.
European Environment Agency, 2023b. Country fact sheet: Italy – air pollution country fact sheet.
Bluhm, R., Polonik, P., Hemes, K.S., Sanford, L.C., Benz, S.A., Levy, M.C., Ricke, K.L., Burney, J.A., 2022. Disparate air pollution reductions during California's COVID-19 economic shutdown. Nat Sustain 5, 509–517.
Boniardi, L., Nobile, F., Stafoggia, M., Michelozzi, P., Ancona, C., 2022. A multi-step machine learning approach to assess the impact of COVID-19 lockdown on NO2 attributable deaths in Milan and Rome, Italy. Environ. Health 21, 1–14.
California Office of Environmental Health Hazard Assessment, 2022. Traffic Impacts.
Cao, X., Liu, X., Hadiatullah, H., Xu, Y., Zhang, X., Cyrys, J., Zimmermann, R., Adam, T., 2022. Investigation of COVID-19-related lockdowns on the air pollution changes in augsburg in 2020. Germany. Atmos Pollut Res 13, 101536.
Chen, G., Tao, J., Wang, J., Dong, M., Li, X., Sun, X., Cheng, S., Fan, J., Ye, Y., Xiao, J., Hu, J., He, G., Sun, J., Lu, J., Guo, L., Li, X., Rong, Z., Zeng, W., Zhou, H., Chen, D., Li, J., Yuan, L., Bi, P., Du, Q., Ma, W., Liu, T., 2021b. Reduction of air pollutants and associated mortality during and after the COVID-19 lockdown in China: Impacts and implications. Environ. Res. 200, 111457.
Chen, K., Wang, M., Huang, C., Kinney, P.L., Anastas, P.T., 2020. Air pollution reduction and mortality benefit during the COVID-19 outbreak in China. Lancet Planet Health 4 (e210-e212).
Chen, C., Warrington, J.A., Dominici, F., Peng, R.D., Esty, D.C., Bobb, J.F., Bell, M.L., 2021a. Temporal variation in association between short-term exposure to fine particulate matter and hospitalisations in older adults in the USA: a long-term time-series analysis of the US Medicare dataset. Lancet Planet Health 5 (e534-e541).
Chen, R., Yin, P., Meng, X., Wang, L., Liu, C., Niu, Y., Lin, Z., Liu, Y., Liu, J., Qi, J., You, J., Kan, H., Zhou, M., 2018. Associations between ambient nitrogen dioxide and daily cause-specific mortality: evidence from 272 Chinese cities. Epidemiology 29, 482–489.
Cyrys, J., Eeftens, M., Heinrich, J., Ampe, C., Armengaud, A., Beelen, R., Bellander, T., Beregszaszi, T., Birk, M., Cesaroni, G., 2012. Variation of NO2 and NOx concentrations between and within 36 European study areas: results from the ESCAPE study. Atmos. Environ. 62, 374–390.
GBD 2019 Risk Factors Collaborators, 2020. Global burden of 87 risk factors in 204 countries and territories, 1990–2019: a systematic analysis for the Global Burden of Disease Study 2019. Lancet 396, 1223–1249.
Giani, P., Castruccio, S., Anav, A., Howard, D., Hu, W., Crippa, P., 2020. Short-term and long-term health impacts of air pollution reductions from COVID-19 lockdowns in China and Europe: a modelling study. Lancet Planet Health 4 (e474-e482).
Grange, S.K., Carslaw, D.C., 2019. Using meteorological normalisation to detect interventions in air quality time series. Sci. Total Environ. 653, 578–588.
Grange, S.K., Carslaw, D.C., Lewis, A.C., Boleti, E., Hueglin, C., 2018. Random forest meteorological normalisation models for Swiss PM 10 trend analysis. Atmos. Chem. Phys. 18, 6223–6239.
Gualtieri, G., Brilli, L., Carotenuto, F., Vagnoli, C., Zaldei, A., Gioli, B., 2020. Quantifying road traffic impact on air quality in urban areas: A Covid19-induced lockdown analysis in Italy. Environ. Pollut. 267, 115682.
Herrmann, H., Wiedensohler, A., Pinxteren, D., Wandinger, U., Tegen, I., Macke, A., 2020. Corona lockdown: The local air quality is always a result of emissions, chemical processes and air pollutant transport.
Hersbach, H., Bell, B., Berrisford, P., Biavati, G., Horányi, A., Muñoz Sabater, J., Nicolas, J., Peubey, C., Radu, R., Rozum, I., Schepers, D., Simmons, A., Soci, C., Dee, D., Thépaut, J-N., 2018. ERA5 hourly data on single levels from 1979 to present. Copernicus Climate Change Service (C3S) Climate Data Store (CDS).
Liu, C., Chen, R., Sera, F., Vicedo-Cabrera, A.M., Guo, Y., Tong, S., Coelho, M.S.Z.S., Saldiva, P.H.N., Lavigne, E., Matus, P., Valdes Ortega, N., Osorio Garcia, S., Pascal, M., Stafoggia, M., Scortichini, M., Hashizume, M., Honda, Y., Hurtado-Díaz, M., Cruz, J., Nunes, B., Teixeira, J.P., Kim, H., Tobias, A., Íñiguez, C., Forsberg, B., Åström, C., Ragettli, M.S., Guo, Y.-L., Chen, B.-Y., Bell, M.L., Wright, C. Y., Scovronick, N., Garland, R.M., Milojevic, A., Kyselý, J., Urban, A., Orru, H., Indermitte, E., Jaakkola, J.J.K., Ryti, N.R.I., Katsouyanni, K., Analitis, A., Zanobetti, A., Schwartz, J., Chen, J., Wu, T., Cohen, A., Gasparrini, A., Kan, H., 2019. Ambient particulate air pollution and daily mortality in 652 cities. N. Engl. J. Med. 381, 705–715.
Ma, Y., Nobile, F., Marb, A., Dubrow, R., Stafoggia, M., Breitner, S., Kinney, P.L., Chen, K., 2024. Short-Term Exposure to Fine Particulate Matter and Nitrogen Dioxide and Mortality in 4 Countries. JAMA Netw. Open 7 (e2354607-e2354607).
Meng, X., Liu, C., Chen, R., Sera, F., Vicedo-Cabrera, A.M., Milojevic, A., Guo, Y., Tong, S., Coelho, M., Saldiva, P.H.N., Lavigne, E., Correa, P.M., Ortega, N.V., Osorio, S., Garcia, Kyselý, J., Urban, A., Orru, H., Maasikmets, M., Jaakkola, J.J.K., Ryti, N., Huber, V., Schneider, A., Katsouyanni, K., Analitis, A., Hashizume, M., Honda, Y., Ng, C.F.S., Nunes, B., Teixeira, J.P., Holobaca, I.H., Fratianni, S., Kim, H., Tobias, A., Íñiguez, C., Forsberg, B., Åström, C., Ragettli, M.S., Guo, Y.L., Pan, S.C., Li, S., Bell, M.L., Zanobetti, A., Schwartz, J., Wu, T., Gasparrini, A., Kan, H., 2021. Short term associations of ambient nitrogen dioxide with daily total, cardiovascular, and respiratory mortality: multilocation analysis in 398 cities. BMJ 372, n534.
Parker, H.A., Hasheminassab, S., Crounse, J.D., Roehl, C.M., Wennberg, P.O., 2020. Impacts of Traffic Reductions Associated With COVID-19 on Southern California Air Quality. Geophys. Res. Lett. 47, e2020GL090164.
Putaud, J.-P., Pisoni, E., Mangold, A., Hueglin, C., Sciare, J., Pikridas, M., Savvides, C., Ondracek, J., Mbengue, S., Wiedensohler, A., 2023. Impact of 2020 COVID-19 lockdowns on particulate air pollution across Europe. Atmos. Chem. Phys. 23, 10145–10161.
Samet, J.M., 2008. Air pollution risk estimates: determinants of heterogeneity. J. Toxic. Environ. Health A 71, 578–582.
Schneider, R., Masselot, P., Vicedo-Cabrera, A.M., Sera, F., Blangiardo, M., Forlani, C., Douros, J., Jorba, O., Adani, M., Kouznetsov, R., 2022. Differential impact of government lockdown policies on reducing air pollution levels and related mortality in Europe. Sci. Rep. 12, 726.
Scortichini, M., Schneider dos Santos, R., De'Donato, F., De Sario, M., Michelozzi, P., Davoli, M., Masselot, P., Sera, F., Gasparrini, A., 2020. Excess mortality during the COVID-19 outbreak in Italy: a two-stage interrupted time-series analysis. Int. J. Epidemiol. 49, 1909–1917.
Shi, Z., Song, C., Liu, B., Lu, G., Xu, J., Van Vu, T., Elliott, R.J., Li, W., Bloss, W.J., Harrison, R.M., 2021. Abrupt but smaller than expected changes in surface air quality attributable to COVID-19 lockdowns. Sci. Adv. 7, eabd6696.
Son, J.-Y., Fong, K.C., Heo, S., Kim, H., Lim, C.C., Bell, M.L., 2020. Reductions in mortality resulting from reduced air pollution levels due to COVID-19 mitigation measures. Sci. Total Environ. 744, 141012.
Venter, Z.S., Aunan, K., Chowdhury, S., Lelieveld, J., 2020. COVID-19 lockdowns cause global air pollution declines. PNAS 117, 18984.
World Health Organization, 2021. WHO global air quality guidelines. Particulate matter (PM2.5 and PM10), ozone, nitrogen dioxide, sulfur dioxide and carbon monoxide.
Xu, M., Sbihi, H., Pan, X., Brauer, M., 2019. Local variation of PM2. 5 and NO2 concentrations within metropolitan Beijing. Atmos. Environ. 200, 254–263.
Yang, J., Wen, Y., Wang, Y., Zhang, S., Pinto, J.P., Pennington, E.A., Wang, Z., Wu, Y., Sander, S.P., Jiang, J.H., 2021. From COVID-19 to future electrification: assessing traffic impacts on air quality by a machine-learning model. Proc. Natl. Acad. Sci. USA 118.
Zhang, J., Lim, Y.-H., Andersen, Z.J., Napolitano, G., Taghavi Shahri, S.M., So, R., Plucker, M., Danesh-Yazdi, M., Cole-Hunter, T., Therming Jørgensen, J., 2022. Stringency of COVID-19 containment response policies and air quality changes: a global analysis across 1851 cities. Environ. Sci. Tech. 56, 12086–12096.
Zheng, H., Li, S., Jiang, Y., Dong, Z., Yin, D., Zhao, B., Wu, Q., Liu, K., Zhang, S., Wu, Y., Wen, Y., Xing, J., Henneman, L.R.F., Kinney, P.L., Wang, S., Hao, J., 2024. Unpacking the factors contributing to changes in PM2.5-associated mortality in China from 2013 to 2019. Environ. Int. 184, 108470.